

Transition-Metal-Stabilized Heavy Tetraphospholide Anions

John A. Kelly, Verena Streitferdt, Maria Dimitrova, Franz F. Westermair, Ruth M. Gschwind, Raphael J. F. Berger, and Robert Wolf*



Cite This: <https://doi.org/10.1021/jacs.2c08754>



Read Online

ACCESS |



Metrics & More

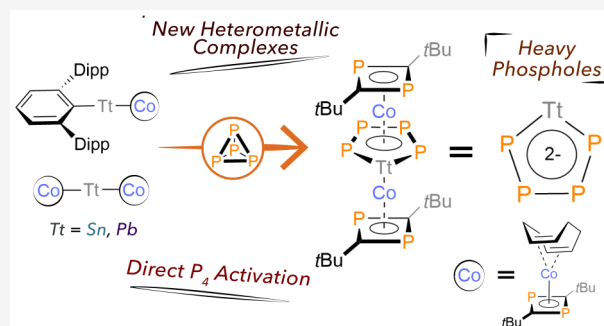


Article Recommendations



Supporting Information

ABSTRACT: Phosphorus analogues of the ubiquitous cyclopentadienyl (Cp) are a rich and diverse family of compounds, which have found widespread use as ligands in organometallic complexes. By contrast, phospholes incorporating heavier group 14 elements (Si, Ge, Sn, and Pb) are hardly known. Here, we demonstrate the isolation of the first metal complexes featuring heavy cyclopentadienyl anions SnP_4^{2-} and PbP_4^{2-} . The complexes $[(\eta^4\text{-}t\text{Bu}_2\text{C}_2\text{P}_2)_2\text{Co}_2(\mu, \eta^5\text{-}\eta^5\text{-P}_4\text{Tt})]$ [Tt = Sn (6), Pb (7)] are formed by reaction of white phosphorus (P_4) with cyclooctadiene cobalt complexes $[\text{Ar}'\text{TtCo}(\eta^4\text{-P}_2\text{C}_2t\text{Bu}_2)(\eta^4\text{-COD})]$ [Tt = Sn (2), Pb (3), $\text{Ar}' = \text{C}_6\text{H}_3\text{-}2,6\{\text{C}_6\text{H}_3\text{-}2,6\text{-}i\text{Pr}_2\}_2$, COD = cycloocta-1,5-diene] and $\text{Tt}\{\text{Co}(\eta^4\text{-P}_2\text{C}_2t\text{Bu}_2)\text{-}(\text{COD})\}_2$ [Tt = Sn (4), Pb (5)]. While the SnP_4^{2-} complex 6 was isolated as a pure and stable compound, compound 7 eliminated Pb(0) below room temperature to afford $[(\eta^4\text{-}t\text{Bu}_2\text{C}_2\text{P}_2)_2\text{Co}_2(\mu, \eta^4\text{-}\eta^4\text{-P}_4)]$ (8), which is a rare example of a tripledecker complex with a P_4^{2-} middle deck. The electronic structures of 6–8 are analyzed using theoretical methods including an analysis of intrinsic bond orbitals and magnetic response theory. Thereby, the aromatic nature of P_5^- and SnP_4^{2-} was confirmed, while for P_4^{2-} , a specific type of symmetry-induced weak paramagnetism was found that is distinct from conventional antiaromatic species.



INTRODUCTION

The diagonal relationship between phosphorus and carbon in the periodic table has inspired the development of a wealth of phosphorus analogues of classical hydrocarbons.¹ Among this family of low-coordinate phosphorus compounds, phospholes take a prominent position due to their relationship to cyclopentadienes.² The sophisticated chemistry of phospholes and the corresponding phospholide anions developed over the last decades has inspired numerous applications in supramolecular chemistry, homogeneous catalysis, and molecular electronics, e.g., in organic light-emitting diodes (OLEDs).^{3–5}

The synthesis of the pentaphospholide anion, P_5^- (A, Figure 1), by Baudler and co-workers was a seminal achievement in phosphole chemistry.⁶ Phospholide A is the pure phosphorus analogue of the ubiquitous cyclopentadienyl anion, Cp^- ($\text{Cp} = \text{C}_5\text{H}_5$). The synthesis of A is achieved by reacting white phosphorus (P_4) with sodium in diglyme or with lithium phosphide in THF. It is noteworthy that the tetraphospholide anion, P_4CH^- , was observed by Baudler in the same reaction mixture but it was not isolated. The crystallographic characterization of the tetraphospholide anion P_4CMes^* (B) was subsequently reported by Ionkin and co-workers.⁷ This anion was isolated as the cesium salt $\text{Cs}[\text{P}_4\text{CMes}^*]$ in a low yield by fractional crystallization from a three-component reaction involving $\text{P}(\text{SiMe}_3)_3$, CsF, and $\text{Mes}^*\text{C}(\text{O})\text{Cl}$ ($\text{Mes}^* = 2,4,6\text{-}t\text{Bu}_3\text{-C}_6\text{H}_2$).

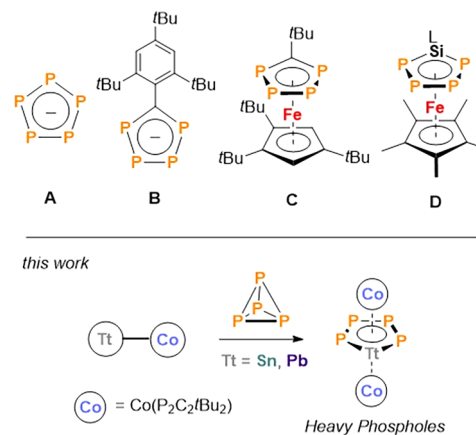


Figure 1. Previous examples of penta- and tetraphospholides (A–D, L = $\text{PhC}(\text{N}t\text{Bu})_2$) and schematic strategy for the synthesis of heavy phospholes reported in this work.

Received: August 17, 2022

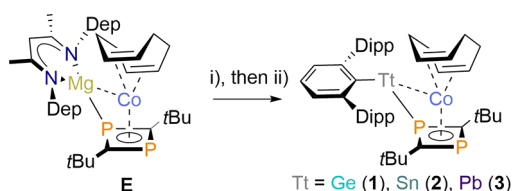
Similarly to Cp, the transition metal coordination chemistry of mono-, di-, tri-, and pentaphospholides is well developed. Notable examples are the pentaphosphaferrocenes $[(C_5R_5)Fe(\eta^5-P_5)]$ ($R = H, Me$), which are outstanding synthons for the assembly of giant supramolecular fullerene analogues.⁴ However, there appears to be only a single example of a tetraphosphole complex in the literature (compound **C**, Figure 1).^{8,9} Tin- and lead-containing aromatic compounds are still scarce.¹⁰ Although heavier group 14 element analogues of the cyclopentadienyl anion, i.e., siloles, germales, and stannoles, are of interest owing to their photophysical properties arising from $\sigma^*-\pi^*$ interactions,^{10f,g,i} analogues of such systems that additionally incorporate a heavier group 15 element such as phosphorus are exceedingly rare. The recently reported compound **D** is a solitary example for a tetraphosphasilole complex.¹¹ Phospholes containing Ge, Sn, or Pb appear to be unknown.

A recent work from our group has successfully utilized the reaction of white phosphorus (P_4) with heterobimetallic complexes to prepare unusual polyphosphorus compounds.^{12,13} Using this strategy, we have now synthesized the heavy tetraphospholide anions SnP_4^{2-} and PbP_4^{2-} . These hitherto unknown π -aromatic molecules are stabilized by the coordination to two cobalt atoms in the triple-decker sandwich compounds $[(\eta^4-tBu_2C_2P_2)_2Co_2(\mu,\eta^5:\eta^5-P_4Tt)]$ [$Tt = Sn$ (**6**), Pb (**7**)]. We describe the structural and spectroscopic characterization of these complexes and analyze the electronic structure of the P_4Tt^{2-} ligands with quantum chemical methods.

RESULTS AND DISCUSSION

Our study commenced with the preparation of the bimetallic tetrel cobaltate complexes $[Ar'TtCo(\eta^4-P_2C_2tBu_2)(\eta^4-COD)]$ [$Tt = Ge$ (**1**), Sn (**2**), Pb (**3**)] used as precursors to our target complexes. Compound **1–3** were prepared by reacting the recently reported magnesium cobaltate salt $[(^{Dep}nacnac)-MgCo(\eta^4P_2C_2tBu_2)(\eta^4-COD)]$ (**E**, $^{Dep}nacnac = CH(DepNCMe)_2$, $Dep = 2,6-Et_2-C_6H_3$) with terphenyl tetrel halides, $[Ar'Tt(\mu-X)]_2$ ($Tt = Ge, X = Cl; Sn, Pb, X = Br$) (Scheme 1). Low temperatures ($-80^\circ C$) are required for

Scheme 1. Synthesis of Compounds **1–3**^a



^aReagents and conditions: (i) $+0.5 [Ar'TtX]_2$ ($Tt = Ge, X = Cl; Sn, Pb, X = Br; Ar' = 2,6-Dipp_2-C_6H_3, Dipp = 2,6-iPr_2-C_6H_3$), toluene, $-78^\circ C$ to r.t., 12 h; (ii) $+Li(^{Dep}nacnac)/-Mg(^{Dep}nacnac)_2, -LiX$, toluene/THF, $-78^\circ C$ to r.t. ($^{Dep}nacnac = CH(DepNCMe)_2, Dep = 2,6-Et_2-C_6H_3$), 12 h.

clean formation of the germanium compound **1**, while for tin and lead, the reactions are selective at ambient temperature. Addition of either $Li(^{Dep}nacnac)$ or $Li(acac)$ ($acac =$ acetyl acetonate) to the reaction mixtures is necessary during workup to convert $[(^{Dep}nacnac)MgX]$ into the *n*-hexane soluble complexes $[Mg(^{Dep}nacnac)_2]$ or $[Mg(^{Dep}nacnac)(acac)]$. Using this procedure, it is possible to isolate **1–3** in moderate

yields as a dark green crystalline powder from concentrated *n*-hexane solutions.

The molecular structures of **1–3** were determined by single-crystal X-ray diffraction. Since all three structures share the same motif, only the molecular structure of **2** is displayed in Figure 2, while those of **1** and **3** are shown in the Supporting

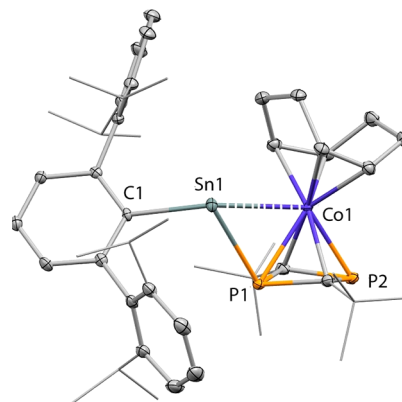


Figure 2. Molecular structure of **2**, with thermal ellipsoids at 30% probability level. Hydrogen atoms are omitted and the *t*Bu and *i*Pr groups drawn in the wire frame model for clarity. Selected bond lengths (Å) and angles (deg): Sn1–Co1 2.9534(5), Sn1–P1 2.6442(7), Sn1–C1 2.252(3), Co1–P1 2.3472(8), Co1–P2 2.2833(8), C1–Sn1–Co1 128.08(6), C1–Sn1–P1 102.17(7).

Information (SI) (Figures S1 and S3). The cobalt atoms feature η^4 -coordinated 1,5-cyclooctadiene and 1,3-diphosphacyclobutadiene ligands, while the tetrel atom (Ge, Sn, or Pb) is in a *pseudo-two-coordinate* environment by terphenyl-substituent and one of the P atoms of the diphosphacyclobutadiene ligand. The Tt–P bond lengths in **1–3** (2.3946(8) Å, 2.6442(7) Å, 2.7402(10) Å, respectively) are similar to those of tertiary phosphine adducts of tetrellylenes.¹⁴ The Tt–Co distances in **1–3** (Ge–Co 2.8434(6) Å, Sn–Co 2.9534(5) Å, Pb–Co: 3.0318(6) Å) are longer than the sum of their covalent radii ($\sum r_{GeCo}$ 2.70 Å, $\sum r_{SnCo}$ 2.89 Å, $\sum r_{PbCo}$ 2.96 Å).¹⁵ These parameters suggest the absence of a covalent metal–metal bond, which is in line with quantum chemical calculations (*vide infra*). By contrast, the previously reported, related cluster compound $(Ar'SnCo)_2$ features strong covalent Sn–Co bonds, which even have partial multiple bond character.¹² The P–C bonds of the diphosphacyclobutadiene ligands are in a close range. It thus appears that the coordination of the tetrel element only has a minor influence on the ligand structure (see SI for a more detailed discussion).

It is noteworthy that although the Tt–Co and Tt–P distances for **1–3** increase down the group, the bond angles are approximately the same (C1–Tt–Co1 127° – 129° , C1–Tt–P1 102° – 103°). As a consequence of the relatively short atomic radius of germanium, the terphenyl substituent and the $Co(P_2C_2tBu_2)(COD)$ unit in **1** are very close to each other resulting in a restricted rotation of the terphenyl ligand around the Tt–P/Tt–C bonds as evidenced by variable temperature (VT) NMR experiments. At room temperature, the NMR spectra of **1** show inequivalence in the 1H and ^{13}C signals for the COD ligand and the *t*Bu groups in agreement with the molecular structure (see SI, Figures S9–15, for details). The 1H NMR spectra for **2** and **3** are far simpler, showing only six signals for the COD ligand and one singlet for the *t*Bu moiety,

indicating a C_s symmetry on the NMR time scale. At lower temperatures, the ^1H NMR signals of **2** and **3** resemble that of **1**. The VT NMR spectrum of **1** at higher temperatures shows only signals corresponding to several decomposition products (at $T > 60$ °C) but not signals corresponding to a C_s symmetric **1**. In contrast, **2** and **3** show no appreciable decomposition up to 110 °C.

The $^{31}\text{P}\{^1\text{H}\}$ NMR spectra for **1–3** are in agreement with the molecular structures. In each case, two doublet signals are observed. Coordination of the P atom to the tetrel center results in a high-field shift of the $^{31}\text{P}\{^1\text{H}\}$ NMR signals ($\delta = -43.5$, -62.3 , and -56.1 ppm for **1**, **2**, and **3**, respectively; see SI) with respect to the signal for the uncoordinated P atom ($\delta = 57.4$, 59.1 , and 59.5 ppm for **1**, **2**, and **3**, respectively). In the case of **2** and **3**, Sn and Pb satellites are present for the signals of the Tt-coordinated P atom ($^1J_{\text{SnP}} = 1050$ Hz, and $^1J_{\text{PbP}} = 1192$ Hz, respectively, see Figures S17 and S25). The corresponding ^{119}Sn and ^{207}Pb NMR signals were observed at 298 K as broad doublets at 1899.7 ppm for **2** (Figure S18) and at 8592 ppm for **3** (Figure S26) and could be unambiguously assigned via the scalar coupling values ($^1J_{\text{PSn}} = 1053$ Hz and $^1J_{\text{PPb}} = 1200$ Hz). At lower temperature (233 K), a significant broadening of the ^{119}Sn NMR signal of **2** was observed (Figure S19), while the ^{207}Pb NMR signal of **3** could not be detected anymore.

Intrinsic bond orbital (IBO), natural bond orbital (NBO) and atoms in molecules (AIM) analyses of DFT calculated electron densities were employed to analyze the bonding situation in **1–3**.^{16,17} The IBO analyses show the expected bond-like localized molecular orbitals. In addition, substantial π -bonding interactions are apparent between the cobalt atom and the π -orbitals of the diphosphacyclobutadiene ligand, which should result in a significant amount of charge transfer (see SI for a more detailed discussion and graphical representations of relevant IBOs). Additionally, there is a delocalized IBO between the tetrel, coordinating phosphorus and cobalt centers, but with low contributions from Co (**1**: Ge (24%) Co (8%) P (59%), **2**: Sn (14%) Co (10%) P (59%), **3**: Pb (13%) Co (10%) P (59%). The Wiberg bond indices for Ge–Co, Sn–Co, and Pb–Co linkages in **1–3** (0.20, 0.15 and 0.13, respectively) are lower than expected for a covalent bond. In line with the results from DFT, the AIM analysis shows bond critical points (BCPs) between cobalt and phosphorus as well as the tetrel atoms and phosphorus (see Figure 3 and SI). However, no BCPs were found between the tetrel atoms and the cobalt center. All these results indicate the presence of only a weak interaction between Tt and Co.

It was also possible to synthesize the homoleptic tin(II) complex $\text{Sn}[\text{Co}(\eta^4\text{-P}_2\text{C}_2\text{tBu}_2)(\text{COD})]_2$ (**4**) by reacting **E** with commercially available $\text{Sn}(\text{acac})_2$ (Figure 4). Single-crystal X-ray diffraction on **4** revealed that the tin atom is coordinated by the two P atoms of the diphosphacyclobutadiene ligands with Sn–P distances (Sn1–P1 2.6490(10), Sn1–P2 2.6484(10) Å) similar to **2** and a P–Sn–P angle of 102.17(7)°. Similar to the structures of **1–3** discussed above, the Sn–Co distances (Sn1–Co2 2.9682(6) and Sn1–Co2 2.9649(7) Å) suggest that there is only a weak interaction between the cobalt atom and tin. The $^{31}\text{P}\{^1\text{H}\}$ NMR spectrum for **4** is comparable to that of **2**, showing two doublet signals ($\delta = 77.2$ and -83.3 ppm, $^2J_{\text{PP}} = 17.4$ Hz). The high-field shifted signal can be assigned to the P atoms coordinated to tin due to the observation of ^{119}Sn satellites ($^1J_{\text{SnP}} = 1067$ Hz; see Figure S32).

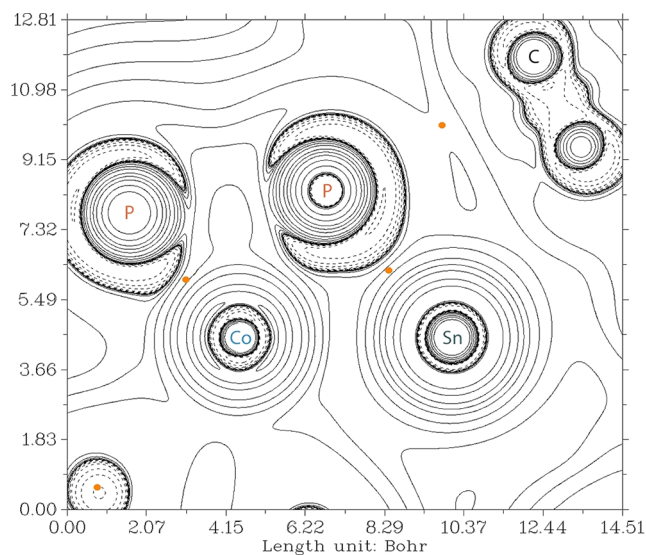


Figure 3. Laplacian contour plot in the P1, P2, Co1, Sn1 plane of **2**; bond critical points are shown as orange dots.

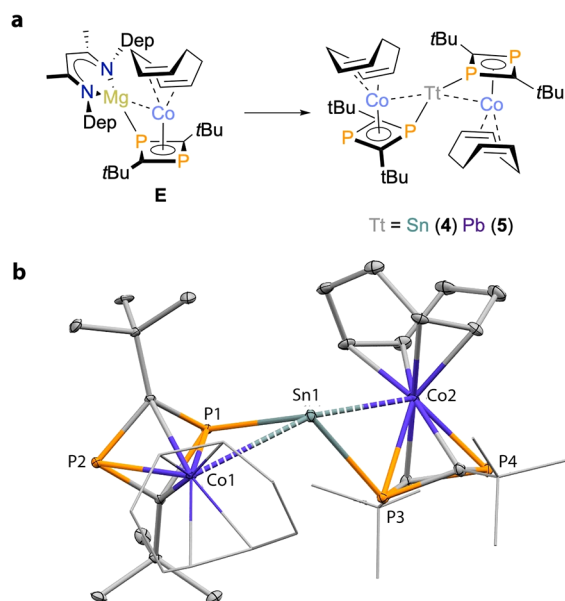


Figure 4. (a) Synthesis of compounds **4** and **5**; reagents and conditions: Tt = Sn: $+\text{Sn}(\text{acac})_2$ (0.5 equiv)/ $-\text{Mg}(\text{D}^{\text{ep}}\text{nacnac})(\text{acac})$, toluene, r.t., 12 h; Tt = Pb: $+\text{Pb}(\text{acac})_2$ (0.5 equiv)/ $-\text{Mg}(\text{D}^{\text{ep}}\text{nacnac})(\text{acac})$, toluene, -30 °C to r.t., 16 h; (b) molecular structure of **4**, with thermal ellipsoids at 30% probability level. Hydrogen atoms are omitted and two *t*Bu groups and the COD ligand drawn in the wire frame model for clarity. Selected bond lengths (Å) and angles (deg): Sn1–Co1 2.9682(6), Sn1–Co2 2.9649(7), Sn1–P1 2.6490(10), Sn1–P2 2.6484(10), Co1–Sn1–Co2 149.374(19), P1–Sn1–P2 100.24(3).

$^{31}\text{P}\{^1\text{H}\}$ NMR analysis of the related reaction of **E** (two equiv) with $\text{Pb}(\text{acac})_2$ indicates the formation of analogous dimetalloplumbylene, $\text{Pb}[\text{Co}(\eta^4\text{-P}_2\text{C}_2\text{tBu}_2)(\eta^4\text{-COD})]_2$ (**5**, see Figure S36). Two doublet signals ($\delta = -65.9$ and 74.1 ppm) are detected of which the high-field shifted signal possesses Pb satellites ($^1J_{\text{PbP}} = 1004$ Hz, $^2J_{\text{PP}} = 19$ Hz). Unfortunately, it was not possible to isolate **5** due to the low thermal stability of the compound. Any isolation attempt resulted in the deposition of a black precipitate (presumably metallic lead).

Having compounds **1–4** in hand, we studied their reactivity toward P_4 to ascertain whether they can be used as precursors to novel polyphosphorus compounds. Reactions between **1** and P_4 were unsuccessful. While no reaction occurs at ambient temperature, heating to 55 °C affords an intractable mixture of products according to $^{31}P\{^1H\}$ NMR spectra (see Figure S15). By contrast, reactions of **2** or **4** with P_4 at elevated temperatures afford the dark red, crystalline compound [(*t*Bu₂C₂P₂)₂Co₂($\mu,\eta^5:\eta^5$ -SnP₄)] (**6**) in each case (Figure 5a).¹⁸ When using **2**, separation of **6** from the unknown

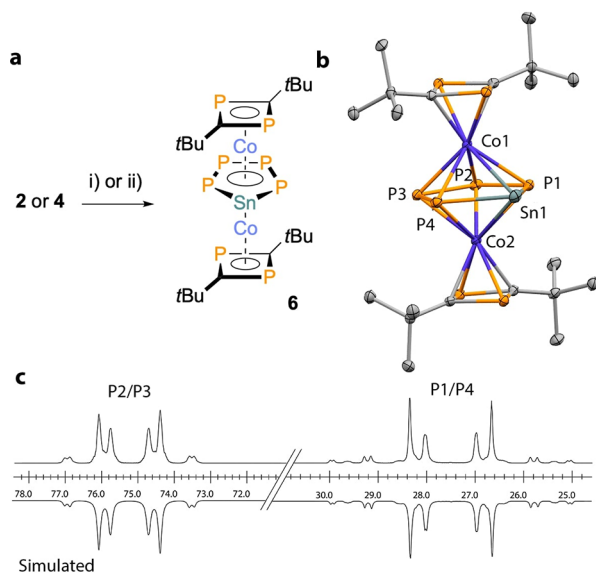


Figure 5. (a) Synthesis of compound **6** via **2** or **4**. Reagents and conditions: (i) **2** (1 equiv), $+P_4$ (1.4 equiv)/–COD, “–Ar’P”, THF, 65 °C, 16 h; (ii) **4** (1 equiv), $+P_4$ (1.2 equiv)/–COD, toluene, 55 °C, 16 h, toluene, r.t., 16 h; (b) molecular structure of **6**, with thermal ellipsoids at 30% probability level. Hydrogen atoms are omitted for clarity. Selected bond lengths (Å) and angles (deg): Sn1–P1 2.5198(8), Sn1–P4 2.5375(9), P1–P2 2.1101(12), P2–P3 2.2296(11), P3–P4 2.1104(12), Co1–Co2 3.050, P1–Sn1–P4 88.17(3), Sn1–P1–P2 118.23(4), P1–P2–P3 107.96(5), P2–P3–P4 107.60(5), P3–P4–Sn1 118.02(4); (c) sections of the measured (upward) and simulated (downward) $^{31}P\{^1H\}$ NMR spectrum of **6**.

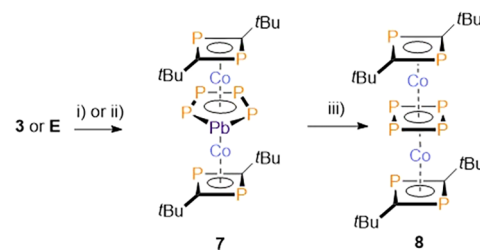
terphenyl containing byproducts proved difficult. Fortunately, the reaction of **4** with P_4 forms **6** selectively at ambient temperature, with 1,5-cyclooctadiene being the only byproduct, making isolation facile and allowing the crystallographic characterization of **6** by single-crystal X-ray diffraction (Figure 5b). The crystallographic analysis reveals the formation of a triple decker complex of two $(\eta^4\text{-P}_2\text{C}_2\text{tBu}_2)\text{Co}$ units and a planar cyclo-SnP_4 middle deck, for which a pronounced alternation of the P–P bond lengths is observed. The P–P bonds adjacent to the Sn atom (P1–P2 2.1101(12) and P3–P4 2.094(4) Å) approach the range for a P=P double bond.¹⁹ The P2–P3 bond length (2.2296(11) Å) suggests the presence of a single bond. The bond lengths between phosphorus and tin (av. P–Sn 2.52865(9) Å) are comparable to the single bonds found in diphosphastannylenes.²⁰

The $^{31}P\{^1H\}$ spectrum of **6** shows one singlet and two multiplets with an integral ratio of 4:2:2. The singlet at $\delta = 67.1$ ppm can be assigned to the P atoms within the $P_2C_2tBu_2$ rings. One of the two multiplet signals ($\delta = 29.6$ and 77.0 ppm), the high-field shifted signal shows coupling to $^{117/119}\text{Sn}$, allowing for its definitive assignment to the P atoms adjacent to

the Sn atom (P1 and P4). Simulation of the $^{31}P\{^1H\}$ spectrum by an iterative fitting procedure gave a $^1J_{PP}$ coupling constant of –434.7 Hz for the P1–P2/P3–P4 pairs, whereas the $^1J_{PP}$ coupling for P2–P3 (magnetically not equivalent) was –289.0 Hz (see Figures S39–S41, Figure 5c). A ^{119}Sn NMR spectrum of **6** shows a broad triplet at $\delta = 339.7$ ppm with a $^1J_{SnP}$ coupling constant of 797 Hz, which is in agreement with the simulated $^{31}P\{^1H\}$ NMR spectrum (see Figures 5c and S41 and Table S1). The line broadening of the ^{119}Sn NMR is likely due to interactions with the quadrupolar ^{59}Co nuclei.²¹

It is noteworthy that the analogous lead compound [(*t*Bu₂C₂P₂)₂Co₂($\mu,\eta^5:\eta^5$ -PbP₄)] (**7**) is formed by reacting **3** with P_4 (Scheme 2). In solution, **7** shows a similar $^{31}P\{^1H\}$

Scheme 2. Synthesis of Compounds **7** and **8**^a



^aReagents and conditions: (i) **3** (1 equiv), $+P_4$ (1 equiv)/–COD, $-P_4\text{Ar}'_2$, “–Ar’P”, toluene, 55 °C, 16 h; (ii) **E** (2 equiv), $+Pb(\text{acac})_2$ (1 equiv), P_4 (1 equiv)/–Mg(^Depnacnac)(acac) (2 equiv), –COD (2 equiv), toluene, –30 °C to r.t., 16 h; (iii) $-Pb$, toluene, storage at r.t.

NMR spectrum as **6** (see the SI for details). However, in contrast to **6**, **7** is unstable at ambient temperature, depositing lead metal and affording a new species, which was identified as [$\text{Co}_2(\text{P}_2\text{C}_2\text{tBu}_2)_2(\mu,\eta^4:\eta^4\text{-P}_4)$] (**8**).

Since no intermediates en route to **6** or **7** were detected by ^{31}P NMR spectroscopy, any mechanistic proposal remains speculative at this point. However, in principle, two distinct scenarios are plausible (i) an initial oxidative addition of P_4 to the group 14 atom (tin or lead) followed by substitution of the cod ligand on cobalt or (ii) the substitution of the cod ligand by P_4 , which would be followed by an insertion of tin(II) or lead(II) into a P–P bond of the resulting tetraphosphido ligand (see SI, Schemes S1 and S2).^{13,22}

While the isolation of **7** and **8** as pure compounds has so far not been possible, their identity was firmly established by single-crystal X-ray analysis and multinuclear NMR spectroscopy (*vide infra*). Additionally, the resonances for the terphenyl– P_4 butterfly compound $\text{D}^{\text{ipp}}\text{Ar}'_2\text{P}_4$ were observed, confirming the fate of the terphenyl ligand attached to the lead center (see Figure S46).²³ Note that these resonances are not present in the $^{31}P\{^1H\}$ NMR spectra for the reaction of **2** with P_4 ; in this case, the fate of the terphenyl substituent remains presently unclear. It should be noted that the one-pot reaction of **E**, $\text{Pb}(\text{acac})_2$, and P_4 also forms **7**, as observed in the $^{31}P\{^1H\}$ NMR spectrum, but only small amounts of crystalline material could be isolated, which were contaminated with $\text{Mg}(\text{D}^{\text{ep}}\text{nacnac})(\text{acac})$.

Similar to complex **6**, the molecular structure of **7** (Figure S6) features a triple-decker structure with a planar cyclo-PbP_4 middle deck. The bond lengths are similar to those observed for **6**, with two short P–P bonds adjacent to the Pb atom (P1–P2 2.1104(12) and P3–P4 2.083(4) Å), and a longer P2–P3 bond in the typical range for P–P single bonds. The P–Pb

distances (av. P–Pb 2.625(3) Å) are in the typical range expected for P–Pb single bonds.²⁰ The ³¹P{¹H} NMR spectrum for **7** is in line with the molecular structure, showing a singlet at $\delta = 67.9$ ppm and multiplet signals at $\delta = 18.5$ and 64.9 ppm (Figure S50).

The molecular structure of **8** (Figure 6) shows the same η^4 -1,3-diphosphacyclobutadiene cobalt moieties as observed in **6**

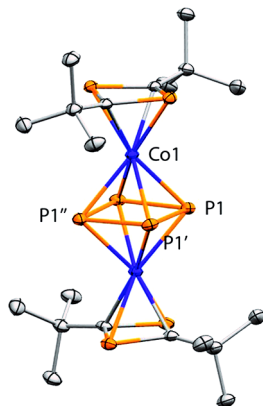


Figure 6. Molecular structure of **8**, with thermal ellipsoids at 30% probability level. Hydrogen atoms are omitted for clarity. Selected bond lengths (Å) and angles (deg): P1–P1' 2.2411(7), Co1–P1 2.3015(6), Co1–Co2 3.377, P1–P1'–P1'' 89.981(1).

and **7**, while the middle deck of the triple-decker structure is a square planar tetraphosphorus ring with equal P–P bond lengths (2.2411(7) Å) and P–P–P bond angles of 90°. The P–P bond length is longer than that found in Cs₂P₄ (2.146(1)/2.1484(9) Å), which also possesses a square planar *cyclo*-P₄ ring.²⁴ Triple-decker sandwich complexes with a *cyclo*-P₄ middle deck have rarely been reported. To our knowledge, the only other examples are [(Cp^RFe)₂(μ , η^4 : η^4 -P₄)]²⁵ and [(Cp^RCo)₂(μ , η^4 : η^4 -P₄)]²⁺ (Cp^R = 1,2,4-*t*Bu₃-C₅H₂).²⁶ Notably, the structure of the iron complex is distinct, featuring a highly distorted, “kite-like” P₄ ring.²⁵ Triple-decker sandwich complexes with a middle deck composed of two separate P₂ units are much more common, such as in [(Cp^RCo)₂(μ , η^2 : η^2 -P₂)]₂ (Cp^R = 1,3-(Me₃Si)₂C₅H₃).^{27,28}

The presence of a triple-decker structure for **8** in solution is confirmed by the ³¹P{¹H} NMR spectrum, which shows a broad singlet at $\delta = 80.8$ ppm for the P₂C₂*t*Bu₂ ring and a quintet at $\delta = 302.6$ ppm corresponding to the *cyclo*-P₄ middle deck. The splitting pattern of the latter signal indicates that the P₄ ring is coupled with the P atoms within the phosphacyclobutadiene rings. Due to the broadness of the singlet for the P₂C₂*t*Bu₂ ring, the ²J_{PP} coupling is not resolved. An iterative fit of the ³¹P{¹H} NMR spectrum gave a ²J_{PP} coupling constant of 10.6 Hz (see the SI for details). The low field signal is in a similar range to Cs₂P₄ ($\delta = 330.3$ ppm) and vastly different from that of [(Cp^RCo)₂(μ , η^2 : η^2 -P₂)]₂ ($\delta = -36.3$) showing two dumbbell P₂ units. The ³¹P NMR spectroscopic data hence indicate that the P₄ ring of **8** remains intact in solution.

In order to gain insight into the electronic structures of the planar polyphosphorus ligands, quantum chemical calculations were performed on the free P₄²⁻, P₅⁻, and TtP₄²⁻ (Tt = Sn, Pb) anions and complexes **6–8** in the gas phase to analyze their electronic properties. The geometry optimization (TPSS-D3BJ/def2-SVP) of the lone dianionic tetraphosphametallole ring, TtP₄²⁻ gives a planar structure with almost identical P–P bond lengths. To analyze the degree of aromaticity or

antiaromaticity, we have undertaken calculations of magnetic response properties. NICS(0) (nucleus independent chemical shifts) calculations indicate that the free molecules P₄Sn²⁻ (–16.0) and PbP₄²⁻ (–15.2) are aromatic. It is apparent that the introduction of the Co moieties in **6** and **7** greatly enhances the aromaticity of the TtP₄ ring. These findings compare well to what was found for the all phosphorus titanocene, [Ti(η^5 -P₅)₂] (–36.8) and P₅⁻ (A, Figure 1, –15.4).²⁹ This trend continues for the P₄ ring within **8** (–3.5) and P₄²⁻ (4.0). Analogous results are obtained when calculating the NICS(1) values (see SI for further details). In addition, we have calculated total molecular currents for P₄²⁻, P₅⁻, and SnP₄²⁻ (at TPSS/def2-TZVP level of theory). According to the magnetic criterion for aromaticity, aromatic molecules maintain a strongly diamagnetic response and antiaromatic molecules maintain a strongly paramagnetic response.²⁹ For a homogeneous magnetic field of strength 1 T perpendicular to the molecular plane, we find total molecular currents of –6.6, 18.9, and 20.2 nA/T for P₄²⁻, P₅⁻, and SnP₄²⁻, respectively. For comparison, molecular currents of 12.0 and –20.0 nA/T were calculated for benzene and cyclobutadiene (in D_{6h} and D_{2h} symmetry, respectively) at the same level of theory. This suggests that P₅⁻ and P₄Sn²⁻ are aromatic species, while P₄²⁻ is nonaromatic or antiaromatic at best.³⁰ Indeed, the paramagnetic response in P₄²⁻ does not emerge from the π system alone but from magnetic $\pi \rightarrow \sigma^*$ (virtual) excitations (see SI for further details).³¹

To investigate how the aromaticity of the [TtP₄]²⁻ is affected by coordination to the cobalt atoms, we have performed a fragment orbital interaction analysis with AMS (formerly known as ADF), and also closely inspected the Kohn–Sham molecular orbitals of **6** and **7** (see SI for details). The two highest occupied π orbitals of [SnP₄]²⁻ are nondegenerate and strongly interact with the empty p_x and p_y orbitals on the cobalt atoms perpendicular to the Co–Co axis. In the complex, the two relevant π orbitals of the [TtP₄]²⁻ ring (the donor orbitals) become almost degenerate. An interesting consequence of this energetic approximation of the π orbitals is that the P–P distances ring become more different in the complex in comparison with the free [TtP₄]²⁻ species.

These results are corroborated by IBO analyses (TPSS D3BJ/def2-SVP level) of the lone dianionic tetraphosphametallole ring, P₄Tt²⁻, which show a delocalized π -system involving the Tt, P1/P3, P2/P4 centers. Figure 7 depicts the multicentered IBOs of SnP₄²⁻ and shows the typical interaction of an aromatic π -system with transition

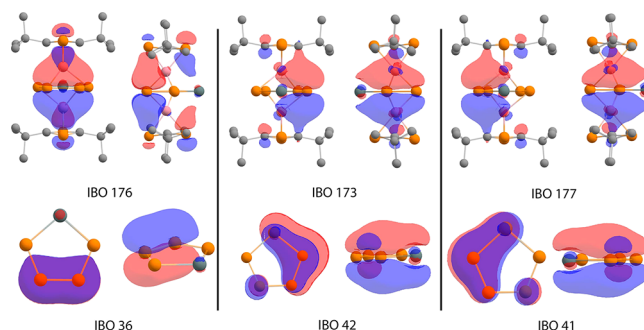


Figure 7. Selected IBOs for compound **6** (above) and the corresponding orbitals for SnP₄²⁻ (below, TPSS-D3BJ/def2-SVP, contour value = 0.03); each IBO is shown from two different perspectives.

metal atoms. The bonding situation of **7** (Figures S74 and S75) and **8** appears to be similar, except the bonding orbitals appear to be more delocalized for **8** (see Figure S76).

CONCLUSION

We have synthesized the first metal complexes of the heavy tetraphospholide anions, SnP_4^{2-} and PbP_4^{2-} . These ligands are of fundamental interest as group 14 analogues of the well-known P_5^- anion. A substantial aromatic character was deduced for P_5^- and SnP_4^{2-} using quantum chemical calculations. The observation of SnP_4^{2-} and PbP_4^{2-} is a milestone in the chemistry of phospholides, while it also bodes well for the preparation of further elusive group 14/group 15 element anions.³² A rich organometallic chemistry is anticipated for these anions, which may offer access to further unusual compounds as shown by the preparation of the phosphorus-rich triple-decker complex **8**. More generally, our work also demonstrates that the activation of P_4 by heterobimetallic complexes has a high utility for the preparation of previously inaccessible (poly-)phosphorus species. We are continuing to explore these avenues.

ASSOCIATED CONTENT

Supporting Information

The Supporting Information is available free of charge at <https://pubs.acs.org/doi/10.1021/jacs.2c08754>.

Full experimental details, X-ray crystallographic data, NMR and UV-vis data, computational details (PDF)

Accession Codes

CCDC 2096444–2096451 contain the supplementary crystallographic data for this paper. These data can be obtained free of charge via www.ccdc.cam.ac.uk/data_request/cif, or by emailing data_request@ccdc.cam.ac.uk, or by contacting The Cambridge Crystallographic Data Centre, 12 Union Road, Cambridge CB2 1EZ, UK; fax: +44 1223 336033.

AUTHOR INFORMATION

Corresponding Author

Robert Wolf – Institute of Inorganic Chemistry, University of Regensburg, 93040 Regensburg, Germany; orcid.org/0000-0003-4066-6483; Email: robert.wolf@ur.de

Authors

John A. Kelly – Institute of Inorganic Chemistry, University of Regensburg, 93040 Regensburg, Germany

Verena Streitferdt – Institute of Organic Chemistry, University of Regensburg, 93040 Regensburg, Germany

Maria Dimitrova – Department of Chemistry, Faculty of Science, University of Helsinki, FI-00014 University of Helsinki, Finland; orcid.org/0000-0002-0711-3484

Franz F. Westermair – Institute of Organic Chemistry, University of Regensburg, 93040 Regensburg, Germany; orcid.org/0000-0002-0197-1664

Ruth M. Gschwind – Institute of Organic Chemistry, University of Regensburg, 93040 Regensburg, Germany; orcid.org/0000-0003-3052-0077

Raphael J. F. Berger – Department for Chemistry and Physics of Materials, Paris-Lodron University Salzburg, 5020 Salzburg, Austria; orcid.org/0000-0002-2284-0540

Complete contact information is available at: <https://pubs.acs.org/10.1021/jacs.2c08754>

Notes

The authors declare no competing financial interest.

ACKNOWLEDGMENTS

We thank Marco Fritz for experimental assistance. Financial support by the Deutsche Forschungsgemeinschaft (RTG IonPairs in Reaction Project 426795949) and the European Research Council (ERC CoG 772299) is gratefully acknowledged. M.D. thanks the Finnish Cultural Foundation for the research grant as well as the Finnish IT-centre for science (CSC) for the computational resources. This paper is dedicated to Oliver Reiser on the occasion of his 60th birthday.

REFERENCES

- (1) (a) Dillon, K. B.; Mathey, F.; Nixon, J. F. *Phosphorus. The carbon copy; from organophosphorus to phospho-organic chemistry*; Wiley: Chichester, 1998; p 1–13. (b) Quin, L. D. Five-membered rings. *Phospholes: Early Literature 1953–1994, Phosphorus-Carbon Heterocyclic Chemistry*; Elsevier Science Ltd: New York, 2001; pp 219–305. (c) Nyulászi, L.; Benkő, Z. Aromatic Phosphorus Heterocycles. *Aromaticity in Heterocyclic Compounds. Topics in Heterocyclic Chemistry*; Springer: Berlin, 2019; Vol. 19, pp 27–81.
- (2) Reviews on phosphole chemistry: (a) Leavitt, F. C.; Manuel, T. A.; Johnson, F. Novel Heterocyclic Pentadienes. *J. Am. Chem. Soc.* **1959**, *81*, 3163. (b) Mathey, F. The organic chemistry of phospholes. *Chem. Rev.* **1988**, *88*, 429. (c) Mathey, F. The chemistry of phospho- and polyphosphacyclopentadiene anions. *Coord. Chem. Rev.* **1994**, *137*, 1. (d) Le Floch, P. Phosphaalkene, phospholyl and phosphinine ligands: New tools in coordination chemistry and catalysis. *Coord. Chem. Rev.* **2006**, *250*, 627. (e) Carmichael, D.; Mathey, F. *New Aspects in Phosphorus Chemistry*; Springer: Heidelberg, 2002; pp 27–51. (f) Ren, Y.; Baumgartner, T. Combining form with function – the dawn of phosphole-based functional materials. *Dalton Trans.* **2012**, *41*, 7792. (g) Duffy, M. P.; Delaunay, W.; Bouit, P.-A.; Hissler, M. π -Conjugated phospholes and their incorporation into devices: components with a great deal of potential. *Chem. Soc. Rev.* **2016**, *45*, 5296. (h) Yamaguchi, S.; Fukazawa, A.; Taki, M. Phosphole P-Oxide-Containing π -Electron Materials: Synthesis and Applications in Fluorescence Imaging. *J. Synth. Org. Chem., Jpn.* **2017**, *75*, 1179. (i) Bezkishko, I. A.; Zagidullin, A. A.; Milyukov, V. A. Chemistry of 1,2-diphospholide anions and 1,2-diphospholes. *Russ. Chem. Bull., Int. Ed.* **2020**, *69*, 435.
- (3) Johannsen, T.; Golz, C.; Alcarazo, M. α -Cationic Phospholes: Synthesis and Applications as Ancillary Ligands. *Angew. Chem., Int. Ed.* **2020**, *59*, 22779.
- (4) Applications of phospholes in (supramolecular) coordination chemistry: (a) Bai, J.; Virovets, A. V.; Scheer, M. Synthesis of Inorganic Fullerene-Like Molecules. *Science* **2003**, *300*, 781. (b) Peresyphkina, E.; Virovets, A.; Scheer, M. Organometallic polyphosphorus complexes as diversified building blocks in coordination chemistry. *Coord. Chem. Rev.* **2021**, *446*, 213995.
- (5) Selected recent literature on phosphole-based functional materials: (a) Su, H.-C.; Fadhel, O.; Yang, C.-J.; Cho, T.-Y.; Fave, C.; Hissler, M.; Wu, C.-C.; Réau, R. Toward Functional π -Conjugated Organophosphorus Materials: Design of Phosphole-Based Oligomers for Electroluminescent Devices. *J. Am. Chem. Soc.* **2006**, *128*, 983. (b) Hong, E. Y.-H.; Poon, C.-T.; Yam, V. W.-W. A Phosphole Oxide-Containing Organogold(III) Complex for Solution-Processable Resistive Memory Devices with Ternary Memory Performances. *J. Am. Chem. Soc.* **2016**, *138*, 6368. (c) Wu, N. M.-W.; Ng, M.; Lam, W. H.; Wong, H.-L.; Yam, V. W.-W. Photochromic Heterocycle-Fused Thieno[3,2-b]phosphole Oxides as Visible Light Switches without Sacrificing Photoswitching Efficiency. *J. Am. Chem. Soc.* **2017**, *139*, 15142. (d) Suter, R.; Benkő, Z.; Bispinghoff, M.; Grützmacher, H. Annulated 1,3,4-Azadiphospholides: Heterocycles with Widely Tunable Optical Properties. *Angew. Chem., Int. Ed.* **2017**, *56*, 11226. (e) Wu, N. M.-W.; Wong, H.-L.; Yam, V. W.-W. Photochromic

benzo[*b*]phosphole oxide with excellent thermal irreversibility and fatigue resistance in the thin film solid state via direct attachment of dithienyl units to the weakly aromatic heterocycle. *Chem. Sci.* **2017**, *8*, 1309.

(6) (a) Baudler, M.; Düster, D.; Ouzounis, D. Beiträge zur Chemie des Phosphors. 172. Existenz und Charakterisierung des Pentaphosphacyclopentadienid-Anions, P_5^- , des Tetraphosphacyclopentadienid-Ions, P_4CH^- , und des Triphosphacyclobutenid-Ions, $P_3CH_2^-$. *Z. Anorg. Allg. Chem.* **1987**, *544*, 87. (b) Baudler, M.; Akpapoglou, S.; Ouzounis, D.; Wasgestian, F.; Meinigke, B.; Budzikiewicz, H.; Münster, H. On the Pentaphosphacyclopentadienide Ion, P_5^- . *Angew. Chem., Int. Ed. Engl.* **1988**, *27*, 280.

(7) Ionkin, A. S.; Marshall, W. J.; Fish, B. M.; Marchione, A. A.; Howe, L. A.; Davidson, F.; McEwen, C. N. Dual Supermesityl Stabilization: A Room-Temperature-Stable 1,2,4-Triphosphole Radical, Sigmatropic Hydrogen Rearrangements, and Tetraphospholide Anion. *Eur. J. Inorg. Chem.* **2008**, *2008*, 2386.

(8) Scheer, M.; Deng, S.; Scherer, O. J.; Sierka, M. Tetraphosphacyclopentadienyl and Triphosphoallyl Ligands in Iron Complexes. *Angew. Chem., Int. Ed.* **2005**, *44*, 3755.

(9) Selected examples of η^5 -polyphospholyl transition metal compounds: (a) Bartsch, R.; Hitchcock, P. B.; Nixon, J. F. First structural characterisation of penta- and hexa-phosphorus analogues of ferrocene. Synthesis, crystal and molecular structure of the air-stable, sublimable iron sandwich compounds $[Fe(\eta^5-C_2R_2P_3)_2]$, and $[Fe(\eta^5-C_3R_3P_2)(\eta^5-C_2R_2P_3)]$ ($R = Bu^t$). *J. Chem. Soc., Chem. Commun.* **1987**, 1146. (b) Nief, F.; Mathey, F.; Ricard, L.; Robert, F. Coordination chemistry of the new 2,3,4,5-tetramethylphospholyl (C_4Me_4P) π -ligand. Crystal and molecular structure of $(\eta^5-C_4Me_4P)_2ZrCl_2 \cdot 1/2C_{10}H_8$. *Organometallics* **1988**, *7*, 921. (c) Bartsch, R.; Hitchcock, P. B.; Nixon, J. F. First example of a 1,2,4-triphosphabuta-1,3-diene complex: synthesis and crystal and molecular structure of $[Co(\eta^5-C_2R_2P_3)(\eta^4-C_2R_2HP_3)]$ ($R = Bu^t$). *J. Chem. Soc., Chem. Commun.* **1988**, 819. (d) Maigrot, N.; Ricard, L.; Charrier, C.; Mathey, F. A New Route to 1,3-Diphospholide Ions. Synthesis and X-Ray Structure Analysis of a 1,3-Diphosphaferrocene. *Angew. Chem., Int. Ed.* **1990**, *29*, 534. (e) Bartsch, R.; Hitchcock, P. B.; Nixon, J. F. η^3 - and η -ligating modes of 1,3-diphosphacyclopentadienyl rings in structurally related molybdenum complexes. Crystal and molecular structure of $[Mo(\eta^5-C_5Me_5)(\eta^3-P_2C_3Bu^t_3)(CO)_2]$ and $[Mo(\eta^3-C_9H_7)(\eta^5-P_2C_3Bu^t_3)(CO)_2]$ ($C_9H_7 = indenyl$). *J. Chem. Soc., Chem. Commun.* **1990**, 472. (f) Ashe, A. J., III; Al-Ahmad, S.; Pilotek, S.; Puranik, D. B.; Elschenbroich, C.; Behrendt, A. Comparison of the Properties of Polymethyl-1,1'-diheteroferrocenes of the Group 15 Elements. *Organometallics* **1995**, *14*, 2689. (g) Feher, R.; Köhler, F. H.; Nief, F.; Ricard, L.; Rossmayer, S. Octamethyl-1,1'-diphosphachromocene: Its Spin Distribution and Oxidation. *Organometallics* **1997**, *16*, 4606. (h) Clark, T.; Elvers, A.; Heinemann, F. W.; Henneemann, M.; Zeller, M.; Zenneck, U. P_6 Manganocene and P_3 Cymantrene: Consequences of the Inclusion of Phosphorus Atoms in Mn-Coordinated Cyclopentadienyl Ligands. *Angew. Chem., Int. Ed.* **2000**, *39*, 2087. (i) Al-Ktaifani, M.; Green, J. C.; Hitchcock, P. B.; Nixon, J. F. Electronic structure of $[M(\eta-P_3C_2Bu^t_2)(CO)_3]$ ($M = Mn$ or Re): a study by photoelectron spectroscopy and density functional calculations. *J. Chem. Soc., Dalton Trans.* **2001**, 1726. (j) Urnëžius, E.; Brennessel, W. W.; Cramer, C. J.; Ellis, J. E.; von Ragué Schleyer, P. A carbon-free sandwich complex $[(P_5)_2Ti]^{2-}$. *Science* **2002**, *295*, 832. (k) Collier, S. J. Product class 24: tetraphospholes. *Science of Synthesis* **2004**, *13*, 763. (l) Cloke, G. N.; Green, J. C.; Hitchcock, P. B.; Nixon, J. F.; Suter, J. L.; Wilson, D. J. Syntheses, structural studies, photoelectron spectra and density functional theory calculations of the "pseudo" tetraphospha-metalloenes $[M(\eta-P_2C_3Bu^t_3)_2]$, ($M = Ni, Pd, Pt$). *Dalton Trans.* **2009**, 1164. (m) Panhans, J.; Heinemann, F. W.; Zenneck, U. Diphospholyl and triphospholyl zirconium π -complexes: Ziegler–Natta oligomerization catalysts and reactive intermediates in P–C cage formation by hydrolysis. *J. Organomet. Chem.* **2009**, *694*, 1223.

(10) (a) Dubac, J.; Laporterie, A.; Manuel, G. Group 14 metalloles. 1. Synthesis, organic chemistry, and physicochemical data. *Chem. Rev.*

1990, *90*, 215. (b) Colomer, E.; Corriu, R. J. P.; Lheureux, M. Group 14 metalloles. 2. Ionic species and coordination compounds. *Chem. Rev.* **1990**, *90*, 265. (c) Saito, M.; Haga, R.; Yoshioka, M.; Ishimura, K.; Nagase, S. The Aromaticity of the Stannole Dianion. *Angew. Chem., Int. Ed.* **2005**, *44*, 6553. (d) Mizuhata, Y.; Sasamori, T.; Takeda, N.; Tokitoh, N. A Stable Neutral Stannaaromatic Compound: Synthesis, Structure and Complexation of a Kinetically Stabilized 2-Stannanaphthalene. *J. Am. Chem. Soc.* **2006**, *128*, 1050. (e) Saito, M.; Sakaguchi, M.; Tajima, T.; Ishimura, K.; Nagase, S.; Hada, M. Dilithioplumbole: A Lead-Bearing Aromatic Cyclopentadienyl Analog. *Science* **2010**, *328*, 339. (f) Cai, Y.; Qin, A.; Tang, B. Z. Siloles in optoelectronic devices. *Mater. Chem. C* **2017**, *5*, 7375. (g) Ramirez y Medina, I.-M.; Rohdenburg, M.; Mostaghimi, F.; Grabowsky, S.; Swiderek, P.; Beckmann, J.; Hoffmann, J.; Dorcet, V.; Hissler, M.; Staubitz, A. Tuning the Optoelectronic Properties of Stannoles by the Judicious Choice of the Organic Substituents. *Inorg. Chem.* **2018**, *57*, 12562. (h) Kaiya, C.; Suzuki, K.; Yamashita, M. A Monomeric Stannabenzene: Synthesis, Structure, and Electronic Properties. *Angew. Chem., Int. Ed.* **2019**, *58*, 7749. (i) Kuwabara, T.; Saito, M. *Siloles, Germales, Stannoles and Plumboses: Comprehensive Heterocyclic Chemistry IV*; Elsevier, 2020; pp 1–35.

(11) Yadav, R.; Simler, T.; Reichl, S.; Goswami, B.; Schoo, C.; Köppe, R.; Scheer, M.; Roesky, P. W. Highly Selective Substitution and Insertion Reactions of Silylenes in a Metal-Coordinated Polyphosphide. *J. Am. Chem. Soc.* **2020**, *142*, 1190.

(12) Hoidn, C. M.; Rödl, C.; McCrea-Hendrick, M. L.; Block, T.; Pöttgen, R.; Ehlers, A. W.; Power, P. P.; Wolf, R. Synthesis of a Cyclic Co_2Sn_2 Cluster Using a Co^- Synthone. *J. Am. Chem. Soc.* **2018**, *140*, 13195.

(13) Kelly, J. A.; Gramüller, J.; Gschwind, R. M.; Wolf, R. Low-oxidation state cobalt–magnesium complexes: ion-pairing and reactivity. *Dalton Trans.* **2021**, *50*, 13985.

(14) (a) Richards, A. F.; Phillips, A. D.; Olmstead, M. M.; Power, P. P. Isomeric Forms of Divalent Heavier Group 14 Element Hydrides: Characterization of $Ar'(H)GeGe(H)Ar'$ and $Ar'(H)_2GeGeAr'-PMe_3$ ($Ar' = C_6H_3-2,6-Dipp_2$; $Dipp = C_6H_3-2,6-Pr'_2$). *J. Am. Chem. Soc.* **2003**, *125*, 3204. (b) Pelzer, S.; Neumann, B.; Stämmler, H.-G.; Ignat'ev, N.; Hoge, B. The Bis(pentafluoroethyl)germylene Trime-thylphosphane Adduct $(C_2F_5)_2Ge-PMe_3$: Characterization, Ligand Properties, and Reactivity. *Angew. Chem., Int. Ed.* **2016**, *20*, 6088. (c) Arp, H.; Baumgartner, J.; Marschner, C.; Müller, T. A Cyclic Disilylated Stannylenes: Synthesis, Dimerization, and Adduct Formation. *J. Am. Chem. Soc.* **2011**, *133*, 5632. (d) Arp, H.; Baumgartner, J.; Marschner, C.; Zark, P.; Müller, T. Dispersion Energy Enforced Dimerization of a Cyclic Disilylated Plumbylene. *J. Am. Chem. Soc.* **2012**, *134*, 6409. (e) Arp, H.; Marschner, C.; Baumgartner, J.; Zark, P.; Müller, T. Coordination Chemistry of Disilylated Stannylenes with Group 10 d^{10} Transition Metals: Silastannene vs Stannylenes Complexation. *J. Am. Chem. Soc.* **2013**, *135*, 7949. (f) Walewska, M.; Hlina, J.; Gaderbauer, W.; Wagner, H.; Baumgartner, J.; Marschner, C. NHC Adducts of Disilylated Germylenes and Stannylenes and Their Coordination Chemistry with Group 11 Metals. *Z. Anorg. Allg. Chem.* **2016**, *642*, 1304.

(15) Cordero, B.; Gómez, V.; Platero-Prats, A. E.; Revés, M.; Echeverría, J.; Cremades, E.; Barragana, F.; Alvarez, S. Covalent radii revisited. *Dalton Trans.* **2008**, 2832.

(16) DFT calculations were performed at the TPSS-D3BJ/def2-TZVP level for **1**, and the TPSS-D3BJ/def2-SVP level with effective core potentials for Co and Sn/Pb for **2** and **3**, respectively.

(17) (a) Tao, J.; Perdew, J. P.; Staroverov, V. N.; Scuseria, G. E. Climbing the Density Functional Ladder: Nonempirical Meta-Generalized Gradient Approximation Designed for Molecules and Solids. *Phys. Rev. Lett.* **2003**, *91*, 146401. (b) Weigend, F.; Ahlrichs, R. Balanced basis sets of split valence, triple zeta valence and quadruple zeta valence quality for H to Rn: Design and assessment of accuracy. *Phys. Chem. Chem. Phys.* **2005**, *7*, 3297. (c) Grimme, S.; Antony, J.; Ehrlich, S.; Krieg, H. A consistent and accurate ab initio parametrization of density functional dispersion correction (DFT-D) for the 94 elements H–Pu. *J. Chem. Phys.* **2010**, *132*, 154104. (d) Grimme,

S.; Ehrlich, S.; Goerigk, L. Effect of the damping function in dispersion corrected density functional theory. *J. Comput. Chem.* **2011**, *32*, 1456. (e) Neese, F. The ORCA program system. *WIREs Comput. Mol. Sci.* **2012**, *2*, 73. (f) Neese, F. Software update: the ORCA program system, version 4.0. *WIREs Comput. Mol. Sci.* **2018**, *8*, e1327.

(18) Note: The reaction of **2** and P₄ in benzene requires three days of heating at 75–80 °C to fully consume **2**; this can be sped up considerably if conducted in THF only needing 16 h at 75 °C. The reaction of **3** and P₄ proceeds to completion within 16 h of heating at 55 °C in benzene.

(19) Allen, F. H.; Kennard, O.; Watson, D. G.; Brammer, L.; Orpen, A. G.; Taylor, R. Tables of bond lengths determined by X-ray and neutron diffraction. Part 1. Bond lengths in organic compounds. *J. Chem. Soc., Perkin Trans.* **1987**, *2*, S1.

(20) (a) Driess, M.; Janoschek, R.; Pritzkow, H.; Rell, S.; Winkler, U. Diphosphanyl- and Diarsanyl-Substituted Carbene Homologues: Germanediyls, Stannanediyls, and Plumbanediyls with Remarkable Electronic Structures. *Angew. Chem., Int. Ed.* **1995**, *34*, 1614. (b) Izod, K.; Evans, P.; Waddell, P. G.; Probert, M. R. Remote Substituent Effects on the Structures and Stabilities of P=E π -Stabilized Diphosphatetrylenes (R₂P)₂E (E = Ge, Sn). *Inorg. Chem.* **2016**, *55*, 10510.

(21) Heinze, K.; Huttner, G.; Zsolnai, L.; Jacobi, A.; Schober, P. Electron Transfer in Dinuclear Cobalt Complexes with “Non-innocent” Bridging Ligands. *Chem. Eur. J.* **1997**, *3*, 732.

(22) Sarkar, D.; Weetman, C.; Munz, D.; Inoue, S. Reversible Activation and Transfer of White Phosphorus by Silyl-Stannylene. *Angew. Chem., Int. Ed.* **2021**, *60*, 3519.

(23) Fox, A. R.; Wright, R. J.; Rivard, E.; Power, P. P. Tl₂[Aryl₂P₄]: A Thallium Complexed Diaryltetraphosphabutadienediide and its Two-Electron Oxidation to a Diaryltetraphosphabicyclobutane, Aryl₂P₄. *Angew. Chem., Int. Ed.* **2005**, *44*, 7729.

(24) Kraus, F.; Aschenbrenner, J. C.; Korber, N. P₄²⁻: A 6 π Aromatic Polyphosphide in Dicesium Cyclotetraphosphide–Ammonia (1/2). *Angew. Chem., Int. Ed.* **2003**, *42*, 4030.

(25) Walter, M. D.; Grunenberg, J.; White, P. S. Reactivity studies on [Cp'FeI]₂: From iron hydrides to P₄-activation. *Chem. Sci.* **2011**, *2*, 2120.

(26) Piesch, M.; Graßl, C.; Scheer, M. Element–Element Bond Formation upon Oxidation and Reduction. *Angew. Chem., Int. Ed.* **2020**, *59* (18), 7154–7160.

(27) (a) Barr, M. E.; Dahl, L. F. Synthesis, stereophysical bonding features, and chemical-electrochemical reactivity of two dimetal-bridging diphosphide cobalt and iron complexes: Co₂(η^5 -C₅Me₅)₂(μ^2 - η^2 -P₂)₂ and Fe₂(η^5 -C₅Me₅)₂(μ^2 - η^2 -P₂)₂. *Organometallics* **1991**, *10*, 3991. (b) Scherer, O. J.; Völmecke, T.; Wolmershäuser, G. Cobalt Complexes with 1,3-Bis(trimethylsilyl)cyclopentadienyl and Substituent-Free P₄ Ligands. *Eur. J. Inorg. Chem.* **1999**, *1999*, 945. (c) Scherer, O. J.; Berg, G.; Wolmershäuser, G. Ligandgesteuerte P₂-Verknüpfung zu einem acyclischen P₄-Liganden. *Chem. Ber.* **1995**, *128*, 635. (d) Bispinghoff, M.; Benkő, Z.; Grützmacher, H.; Delgado Calvo, F.; Caporali, M.; Peruzzini, M. Ruthenium mediated halogenation of white phosphorus: synthesis and reactivity of the unprecedented P₄Cl₂ moiety. *Dalton Trans.* **2019**, *48*, 3593.

(28) A related tris(diphosphacyclobutadiene) tripledecker complex [Co₂(η^4 -tBu₂)₂(μ - η^4 - η^4 -P₂C₂tBu₂)] was recently prepared by a completely different route: Roedel, C.; Hierlmeier, G.; Wolf, R. A homoleptic tris(diphosphacyclobutadiene) tripledecker sandwich complex. *Chem. Commun.* **2022**, DOI: 10.1039/D2CC04601F.

(29) Liu, Z.-Z.; Tian, W.-Q.; Feng, J.-K.; Zhang, G.; Li, W.-Q. Theoretical Study on Structures and Aromaticities of P₅⁻ Anion, [Ti(η^5 -P₅)]⁻ and Sandwich Complex [Ti(η^5 -P₅)₂]²⁻. *J. Phys. Chem. A* **2005**, *109*, 5645.

(30) Sundholm, D.; Dimitrova, M.; Berger, R. J. F. Current density and molecular magnetic properties. *Chem. Commun.* **2021**, *57*, 12362.

(31) Viel, A.; Berger, R. J. F. The symmetry principle of antiaromaticity. *Z. Naturforsch., B. Chem. Sci.* **2020**, *75*, 327.

(32) Figueroa and Cummins have reported the preparation of EP₂ ligands in niobium complexes: Figueroa, J. S.; Cummins, C. C. Triatomic EP₂ Triangles (E = Ge, Sn, Pb) as μ - η^3 , η^3 -Bridging Ligands. *Angew. Chem., Int. Ed.* **2005**, *44*, 4592.

Recommended by ACS

Cation- and Anion-Mediated Supramolecular Assembly of Bismuth and Antimony Tris(3-pyridyl) Complexes

Álvaro García-Romero, Raúl García-Rodríguez, *et al.*

DECEMBER 09, 2021
INORGANIC CHEMISTRY

READ 

Acid/Base-Free Acyclic Anionic Oxoborane and Iminoborane Bearing Diboryl Groups

Manling Bao, Yuanting Su, *et al.*

JULY 10, 2022
INORGANIC CHEMISTRY

READ 

Synthesis, Structure, and Reactivity of a Superbulky Low-Valent β -Diketimate Al(I) Complex

Samuel Grams, Sjoerd Harder, *et al.*

OCTOBER 04, 2022
ORGANOMETALLICS

READ 

Switching from Heteronuclear Allyl Cations to Vinyl Cations by Using a Chemical Charge Trap

Julia Krüger, Stephan Schulz, *et al.*

DECEMBER 23, 2021
INORGANIC CHEMISTRY

READ 

Get More Suggestions >